

# Superoxide Dismutase-Based Third-Generation Biosensor for Superoxide Anion

Yang Tian, Lanqun Mao, Takeyoshi Okajima, and Takeo Ohsaka\*

Department of Electronic Chemistry, Interdisciplinary Graduate School of Science and Engineering, Tokyo Institute of Technology, 4259 Nagatsuta, Midori-ku, Yokohama 226-8502, Japan

**A third-generation biosensor for superoxide anion ( $O_2^-$ ) was developed by immobilizing superoxide dismutase (SOD) on a self-assembled monolayer of cysteine on gold electrode; i.e., a SOD/cysteine-modified gold electrode (SOD/Cys/Au) was fabricated. A rapid and direct electron transfer of SOD was realized at the gold electrode by using the cysteine molecule as an electron-transfer promoter. The promoted direct electron transfer of SOD and biomolecular recognition by the exploitation of specific and significant enzyme–substrate reactivity of SOD toward  $O_2^-$  combined with the low operating potential enabled a sensitive measurement of  $O_2^-$ . At SOD/Cys/Au,  $O_2^-$  could be specifically oxidized and reduced to  $O_2$  and hydrogen peroxide, respectively, through the inherent catalytic reaction of SOD. This allowed us to measure  $O_2^-$  by polarizing the electrode both anodically and cathodically. We could successfully measure  $O_2^-$  by suitably polarizing the electrode, typically at 300 and  $-200$  mV versus Ag/AgCl without the virtual interference from physiological levels of  $H_2O_2$ , ascorbic acid, uric acid, and metabolites of neurotransmitters. The response mechanism of SOD/Cys/Au to  $O_2^-$  and its sensor characteristics are also presented and discussed.**

Superoxide anion ( $O_2^-$ ), the primary species of the so-called reactive oxygen species (ROS), is generated as a reduced intermediate of molecular oxygen in significant quantities in a variety of biological systems. Under normal physiological conditions,  $O_2^-$  undergoes disproportionation by noncatalytic and enzymatic reactions, resulting in a rather low and undetectable endogenous physiological concentration. However, increases in the activity of  $O_2^-$  occur in response to traumatic brain injury<sup>1,2</sup> ischemia–reperfusion and hypoxia, and  $O_2^-$  may be involved in the etiology of aging, cancer, and progressive neurodegenerative diseases such as Parkinson's disease.<sup>3–6</sup> Actually,  $O_2^-$  is not so reactive in itself, but it can easily turn to hydroxyl radical, which

is the most potent radical, by the Fenton reaction in the presence of metal ions such as  $Fe^{2+}$  and  $Cu^{2+}$ .<sup>7–9</sup> In addition, recent attempts have been focused on the interplay of nitric oxide and  $O_2^-$  and have shown that  $O_2^-$  reacts with NO to produce hydroxyl radical and peroxynitrite, which has also been implicated in the pathogenesis of atherosclerosis and neurodegenerative diseases.<sup>10,11</sup> These findings suggest that  $O_2^-$  is of great importance in the determination of cellular damage, and thus, a specific and sensitive method for durable and reliable measurements of  $O_2^-$  would facilitate the investigations on the pathology and physiology of diseases relevant to ROS and on free-radical biochemistry.

Over past decades many attempts have been made to develop methods for the detection of  $O_2^-$ , and some techniques have been demonstrated to be reliable for this purpose, such as spectrophotometry and electron spin resonance.<sup>12–16</sup> Electrochemical methods have also drawn extensive attention because they have more advantages such as direct detection, high sensitivity, measurement in vivo, and so on. There have been many papers about the electrochemical measurements of  $O_2^-$ .<sup>17–32</sup> Of the hitherto-reported electrochemical methods, the third-generation biosensor

\* Author to whom correspondence should be addressed. Tel: +81-45-924-5404. Fax: +81-45-924-5489. E-mail: ohsaka@echem.titech.ac.jp.

- (1) Kontos, H. A.; Wei, E. P. *J. Neurosurg.* **1986**, *64*, 803–807.
- (2) Globus, M. Y.; Alonso, O.; Dietrich, W. A.; Busto, R.; Ginsberg, M. D. *J. Neurochem.* **1995**, *65*, 1704–1711.
- (3) Hall, E. D.; Braughler, J. M. *Free Radical Biol. Med.* **1989**, *6*, 303–313.
- (4) Vanella, A.; Di Giacomo, C.; Sorrenti, V.; Russo, A.; Castorina, C.; Campisi, A.; Renis, M.; Perez-Polo, J. R. *Neurochem. Res.* **1993**, *18*, 1337–1340.
- (5) Floyd, R. A. *FASEB J.* **1990**, *4*, 2587–2597.
- (6) Ames, B. N.; Shigenaga M. K.; Hagen, J. M. *Proc. Natl. Acad. Sci. U.S.A.* **1993**, *90*, 7915–7922.

- (7) Halliwell, B. *J. Neurochem.* **1992**, *59*, 1609–1623.
- (8) Benzi, G.; Moretti, A. *Free Radical Biol. Med.* **1995**, *19*, 77–101.
- (9) Stohs, S. J.; Bagchi, D. *Free Radical Biol. Med.* **1995**, *18*, 321–336.
- (10) Beckman, J. S.; Kippenol, W. H. *Am. J. Physiol.* **1995**, *271*, 1424–1437.
- (11) Gross, S. S.; Wolin, M. S. *Annu. Rev. Physiol.* **1995**, *57*, 737–769.
- (12) Zweier, J. L.; Flaherty, J. H.; Weisfeldt, M. L. *Proc. Natl. Acad. Sci. U.S.A.* **1987**, *84*, 1404–1407.
- (13) Ohara, Y.; Peterson, T. E.; Harrison, D. G. *J. Clin. Invest.* **1993**, *91*, 2546–2551.
- (14) Vasquez-Vivar, J.; Hogg, N.; Pritchard, K. A.; Kalyanaraman, B. *FEBS Lett.* **1997**, *403*, 127–130.
- (15) Zhang, H.; Joseph, J.; Vasquez-Vivar, J.; Karoui, H.; Nsanumuhire, C.; Martasek, P.; Tordo, P.; Kalyanaraman, B. *FEBS Lett.* **2000**, *473*, 58–62.
- (16) Ohyashiki, T.; Nunomura, M.; Katoh, T. *Biochim. Biophys. Acta* **1999**, *1421*, 131–139.
- (17) Tanaka, K.; Kobayashi, F.; Isogai, Y.; Iizuka, T. *Bioelectrochem. Bioenerg.* **1991**, *26*, 413–421.
- (18) Privat, C.; Trevin, S.; Bedioui, F.; Devynck, J. J. *Electroanal. Chem.* **1997**, *436*, 261–265.
- (19) Lisdat, F.; Ge, B.; Ehrentreich-Forster, E.; Reszka, R.; Scheller, F. W. *Anal. Chem.* **1999**, *71*, 1359–1365.
- (20) Tammeveski, K.; Tenno, T.; Mashirin, A. A.; Hillhouse, E. W.; Manning, P.; McNeil, C. J. *Free Radical Biol. Med.* **1998**, *25*, 973–978.
- (21) Chen, J.; Wollenberger, U.; Lisdat, F.; Ge, B.; Scheller, F. W. *Sens. Actuators, B* **2000**, *70*, 115–120.
- (22) Xue, J.; Xian, X.; Ying, X.; Chen, J.; Wang, L.; Jin, L. *Anal. Chim. Acta* **2000**, *405*, 77–85.
- (23) Scheller, W.; Jin, W.; Ehrentreich-Forster, E.; Ge, B.; Lisdat, F.; Buttemeier, R.; Wollenberger, U.; Scheller, F. W. *Electroanalysis* **1999**, *11*, 703–706.
- (24) Gobi, K. V.; Mizutani, F. *J. Electroanal. Chem.* **2000**, *484*, 172–181.
- (25) McNeil, C. J.; Athey, D.; Ho, W. O. *Biosens. Bioelectron.* **1995**, *10*, 75–83.
- (26) Lvovich, V.; Scheeline, A. *Anal. Chem.* **1997**, *69*, 454–462.

proposed to be based on a direct electrochemical redox reaction of enzyme is the most attractive in biosensor development due to the simple procedure required for sensor design (which results in miniaturization) and the high sensitivity, and thus developing the third-generation biosensor is a challenging analytical problem. In 1982, Taniguchi et al. reported for the first time a direct redox reaction of cytochrome *c* (Cyt. *c*) at a modified gold electrode and demonstrated that the electron transfer of Cyt. *c* could be promoted by molecular monolayers of electrode modifiers such as 4,4'-bipyridyl and bis(4-pyridyl) disulfide.<sup>33,34</sup> Since then, the direct electrochemistry of Cyt. *c* has been extensively studied<sup>35–37</sup> and much effort has been paid to the design of a third-generation biosensor for  $O_2^-$  based on the reaction of  $O_2^-$  with Cyt. *c*.<sup>19,20,23,24,27,37,38</sup> As expected, the Cyt. *c*-based  $O_2^-$  sensors have been demonstrated to have a good sensitivity for the measurement of  $O_2^-$  and to be free from interference from ascorbic acid (AA) and uric acid (UA) due to the low operating potential. However, the inherent property of Cyt. *c* as a peroxidase to reduce  $H_2O_2$ <sup>24,37</sup> makes the sensor suffer from interference from  $H_2O_2$  either in the XOD/xanthine  $O_2^-$  generating system or endogenously coexisting in biological systems. This greatly limited the application of Cyt. *c*-based  $O_2^-$  sensors for detection of  $O_2^-$  in biological systems although the peroxidase activity of Cyt. *c* has been reported to be controlled by electrode design.<sup>24</sup> More essentially, Cyt. *c* is not an enzyme specific for  $O_2^-$  although its reduction by  $O_2^-$  is possible, and therefore, the activity and specificity of Cyt. *c* toward  $O_2^-$  are significantly low compared with superoxide dismutase (SOD), which is an enzyme specific for  $O_2^-$  dismutation<sup>26,28,29</sup> (vide infra).

SOD has been well addressed for the dismutation of  $O_2^-$  to  $O_2$  and  $H_2O_2$  with strong activity and great specificity, and this strategy was recently used to develop amperometric sensors for  $O_2^-$  measurements.<sup>26,28–30,32,39</sup> However, the sensors reported in the literature are mainly based on the detection of  $H_2O_2$  produced from the  $O_2^-$  dismutation catalyzed by SOD, in which such a high potential is required for the oxidation of  $H_2O_2$  that it causes the simultaneous oxidation of some coexisting electroactive species in biological samples, e.g., AA and UA. More importantly,  $H_2O_2$  is a metabolite of the degradation of  $O_2^-$  as well as a product from the enzymatic reaction of endogenous oxidases such as monoamine oxidase and L-amino acid oxidase.<sup>7,8</sup> Thus, when these sensors

are used in biological systems, it is necessary to differentiate between the signals from  $H_2O_2$  produced from SOD catalytic dismutation of  $O_2^-$  and from  $H_2O_2$  endogenously present in biological systems. The interference from the coexisting electroactive species and endogenous  $H_2O_2$  greatly limited the practical applications of the sensors<sup>38,40</sup> previously proposed for determination of  $O_2^-$  in biological systems. At this point, the two-channel sensor proposed by Lvovich and Scheeline, which is capable of simultaneous detection of  $O_2^-$  and  $H_2O_2$ , is worthy of notice.<sup>26</sup> However, the difference in amperometric response of two independent electrodes to  $H_2O_2$  makes it difficult to obtain a net response of  $O_2^-$  at the sensor for both  $O_2^-$  and  $H_2O_2$ .

Recently, we realized a direct electrochemistry of SOD at a cysteine-modified electrode and demonstrated that the promoted direct electron transfer is associated with the redox reaction of the copper complex moiety, which is also responsible for the dismutation activity.<sup>41</sup> In this work, by utilizing the direct electrochemistry of SOD, we have developed for the first time a third-generation biosensor for  $O_2^-$ . The low detection limit and high specificity against AA, UA,  $H_2O_2$ , and metabolites of some neurotransmitters suggest the potential application of the sensor for the practical detection of  $O_2^-$  in biological systems.

## EXPERIMENTAL SECTION

**Reagents.** L-Cysteine was obtained from Kanto Chemical Co. (Tokyo, Japan), and its aqueous solution was freshly prepared and deoxygenated by bubbling pure nitrogen gas for at least 30 min prior to use. Bovine erythrocyte copper–zinc SOD ( $Cu_2ZnSOD$ , EC 1.15.1.1) was purchased from Wako Pure Chemical Industries Ltd. (Tokyo, Japan) and used as received. Xanthine oxidase (XOD, EC 1.1.3.22, buttermilk source) and catalase (EC 1.11.1.6) were purchased from Sigma Chemical Co. (St. Louis, MO.) and used as supplied. 5-Hydroxyindole-3-acetic acid (5-HIAA), 3,4-dihydroxyphenylacetic acid (DOPAC), and homovanillic acid (HVA) were purchased from Sigma. Xanthine, uric acid,  $H_2O_2$ , L-ascorbic acid, diethyldithiocarbamate (DDC), and other chemicals were of analytical grade and were purchased from Kanto Chemical Co. Cu-free derivative  $E_2ZnSOD$  (E = empty, denoted as apo-SOD) was prepared according to the method described by Cocco et al.<sup>44</sup> Briefly, DDC was added into 0.1 M potassium phosphate buffer (pH 7.4) containing 0.28 mM  $Cu_2ZnSOD$ . The mixture was incubated at 37 °C until no further increase in the absorption strength at 450 nm due to the DDC–Cu complex was observed (~1.5 h at a DDC/ $Cu_2ZnSOD$  ratio of 5:1). The yellow solution was centrifuged at 39000g for 30 min, and the colorless supernatant was then exhaustively dialyzed against deionized water to remove the DDC–Cu complex. Deionized water (Milli-Q system, Millipore) was used to prepare all aqueous solutions.

**Preparation of the SOD-Immobilized Gold Electrode.** Polycrystalline gold electrodes (1.6 mm in diameter, BAS, West

- (27) Campanella, L.; Persi, L.; Tomassetti, M. *Sens. Actuators, B* **2000**, *68*, 351–359.
- (28) Mesaros, S.; Vankova, Z.; Mesarosova, A.; Tomcik, P.; Grunfeld, S. *Bioelectrochem. Bioenerg.* **1998**, *46*, 33–37.
- (29) Mesaros, S.; Vankova, Z.; Grunfeld, S.; Mesarosova, A.; Malinski, T. *Anal. Chim. Acta* **1998**, *358*, 27–30.
- (30) Campanella, L.; Favero, G.; Persi, L.; Tomassetti, M. J. *Pharm. Biomed. Anal.* **2000**, *23*, 69–76.
- (31) Song, M. I.; Bier, F. F.; Scheller, F. W. *Bioelectrochem. Bioenerg.* **1995**, *38*, 419–422.
- (32) Descroix, S.; Bedioui, F. *Electroanalysis* **2001**, *13*, 524–528.
- (33) Taniguchi, I.; Toyosawa, K.; Yamaguchi, H.; Yasukouchi, K. J. *Electroanal. Chem.* **1982**, *140*, 187–193.
- (34) Taniguchi, I.; Toyosawa, K.; Yamaguchi, H.; Yasukouchi, K. J. *Chem. Soc., Chem. Commun.* **1982**, 1032–1033.
- (35) Collinson, M.; Bowden, E. F.; Tarloc, M. J. *Langmuir* **1992**, *8*, 1247–1250.
- (36) Cooper, J. M.; Greenough, K. R.; McNeil, C. J. J. *Electroanal. Chem.* **1993**, *347*, 267–275.
- (37) Lotzbeyer, T.; Schuhmann, W.; Schmidt, H. *Sens. Actuators, B* **1996**, *33*, 50–54.
- (38) McNeil, C. J.; Greenough, K. R.; Weeks, P. A.; Self, C. H.; Cooper, J. M. *Free Radical Res. Commun.* **1992**, *17*, 399–406.
- (39) Tanaka, K.; Muto, Y. *Bioelectrochem. Bioenerg.* **1992**, *29*, 143–147.

- (40) Manning, P.; McNei, C. J.; Cooper, J. M.; Hillhouse, E. W. *Free Radical Biol. Med.* **1998**, *24*, 1304–1309.
- (41) Tian, Y.; Shioda, M.; Kasahara, S.; Okajima, T.; Mao, L.; Hisaboli, T.; Ohsaka, T. *Biochim. Biophys. Acta* **2002**, *1569*, 151–158.
- (42) Wu, X.; Meng, X.; Wang, Z.; Zhang, Z. *Chem. Lett.* **1999**, *12*, 1271–1272.
- (43) Meng, X.; Wu, X.; Wang, Z.; Cao, X.; Zhang, Z. *Bioelectrochemistry* **2001**, *54*, 125–129.
- (44) Cocco, D.; Calabrese, L.; Rigo, A.; Marmocchi, F.; Rotitlio, G. *Biochem. J.* **1981**, *199*, 675–680.

Lafayette, IN) were polished with aqueous slurries of successively finer alumina powder (down to 0.06  $\mu\text{m}$ ) on a polishing microcloth and were sonicated for 10 min in water. Electrodes were then pretreated electrochemically in 0.05 M  $\text{H}_2\text{SO}_4$  by potential cycling in the potential range of  $-0.2$  to  $+1.5$  V at a potential scan rate of  $10 \text{ V s}^{-1}$  until the cyclic voltammogram characteristic for a clean gold electrode was obtained (typically 10 min.). According to the standard procedure for preparing the self-assembled monolayers (SAMs) of thiols and disulfides on a gold electrode,<sup>45,46</sup> a cysteine-SAM-modified Au electrode (denoted as Cys/Au) was prepared by dipping the freshly prepared Au electrode in 1 mM cysteine solution for 10 min and then rinsing the electrode carefully with deionized water to remove the nonchemisorbed cysteine. SOD (or apo-SOD) was immobilized on the cysteine-modified Au electrode by soaking it in 25 mM phosphate buffer containing 0.56 mM SOD (or apo-SOD) for 30 min. The thus-prepared SOD (or apo-SOD)/Cys-modified Au was then rinsed with deionized water and stored at 4 °C while not being used. Hereafter, these electrodes modified with SOD and apo-SOD will be referred to as SOD/Cys/Au and apo-SOD/Cys/Au, respectively.

**Electrochemical Measurements.** Electrochemical measurements were performed in a conventional two-compartment three-electrode cell with computer-controlled BAS 100 B/W (BAS) or CHI Electrochemical Analyzer (CHI Inc.). SOD/Cys/Au or apo-SOD/Cys/Au was used as the working electrode, with a platinum spiral wire as the counter electrode and a Ag/AgCl electrode (saturated with KCl) as the reference electrode. The working electrode and the counter electrode were separated with a porous glass. The electrochemical measurements were carried out in 25 mM phosphate-buffered solution (PBS, pH 7.4).  $\text{O}_2^-$  was generated by the addition of aliquots of xanthine to PBS ( $\text{O}_2^-$ -saturated) containing 0.002 unit of XOD. The amount of  $\text{O}_2^-$ -saturated produced from the univalent reduction of oxygen by XOD<sup>47</sup> in the present experimental condition, i.e., the rate of  $\text{O}_2^-$  generation, was determined by examining the reduction of ferricytochrome *c* spectrophotometrically<sup>13,28,29,48</sup> and using the extinction coefficient ( $21.1 \text{ mM}^{-1} \text{ cm}^{-1}$ )<sup>13</sup> of ferrocycytochrome *c* at 550 nm. The yield of  $\text{O}_2^-$  was 26% of the total xanthine present in the reaction in the range of xanthine concentration from 10 to 200 nM.  $\text{O}_2^-$  was detected with SOD/Cys/Au by holding its electrode potential at 300 or  $-200$  mV. Electrolyte solution containing 0.002 unit of XOD was stirred with a magnetic stirrer at 200 rpm. Aliquots of xanthine standard were successively pipetted to the solution to measure the current response stepwise after a smooth background response was obtained. All experiments were carried out at  $25 \pm 0.5$  °C.

## RESULTS AND DISCUSSION

**Electrochemical Behavior of SOD/Cys/Au in the Absence and Presence of  $\text{O}_2^-$ .** Figure 1 depicts typical cyclic voltammograms (CVs) of Cys/Au and SOD/Cys/Au in 25 mM PBS (pH 7.4) at  $100 \text{ mV s}^{-1}$ . A well-defined reversible redox wave with a formal potential,  $E^\circ$ , of 60 mV was observed at SOD/Cys/Au,

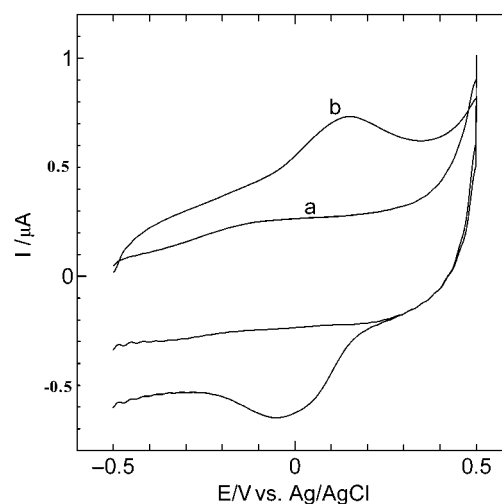


Figure 1. CVs of (a) Cys/Au and (b) SOD/Cys/Au in 25 mM PBS at  $100 \text{ mV s}^{-1}$ . The surface coverages of cysteine and SOD were  $8.1 \times 10^{-10}$  and  $1.5 \times 10^{-11} \text{ mol cm}^{-2}$ , respectively.

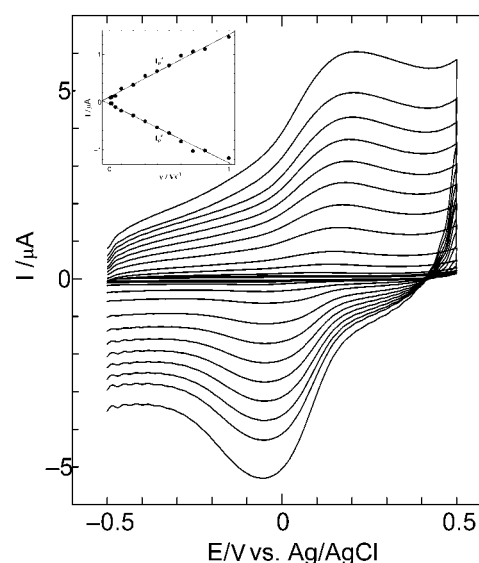


Figure 2. CVs of SOD/Cys/Au in PBS solution at scan rates of 10, 20, 50, 100, 200, 300, 400, 500, 600, 700, 800, and  $1000 \text{ mV s}^{-1}$ . The inset shows the relationship between peak current and scan rate.

while no voltammetric response was obtained at Cys/Au under the same conditions. As addressed previously,<sup>38</sup> the direct electron transfer of SOD at a bare gold electrode is very slow and thus it has not been observed actually, but it could be considerably promoted by use of a cysteine monolayer, in which the SAM of cysteine bridges between SOD and the electrode and functions as the so-called promoter for the electron-transfer reaction of SOD.<sup>41–43</sup> In addition, the promoted direct electron transfer of SOD was found to be associated with the redox reaction of the copper active site in native SOD.<sup>41</sup>

A typical example of the CVs of SOD/Cys/Au in PBS at various sweep rates is shown in Figure 2. The CVs remained essentially unchanged on consecutive potential cycling, demonstrating that SOD is stably confined on the SAM of cysteine. In addition, we found that both the anodic and cathodic peak currents ( $I_p^a$  and  $I_p^c$ ) vary linearly with potential scan rate ( $\nu$ ) in the range of  $10$ – $1000 \text{ mV s}^{-1}$  (the inset in Figure 2) and the ratio of  $I_p^c/I_p^a$  at a given  $\nu$  is nearly unity. This cysteine-promoted rapid and direct

(45) Finklea, H. O. In *Electroanalytical Chemistry*; Bard, A. J., Rubinstein, I., Eds.; Marcel Dekker: New York, 1996; Vol. 19, p 109.

(46) Ulman, A. *An Introduction to Ultrathin Organic Films: From Langmuir–Blodgett to Self-Assembly*; Academic Press: San Diego, CA, 1991.

(47) Olson, J. S.; Ballou, D. P.; Palmer, G.; Massey, V. *J. Biol. Chem.* **1974**, *249*, 4350–4362.

(48) Fridovich, I. *J. Biol. Chem.* **1970**, *245*, 4053–4057.



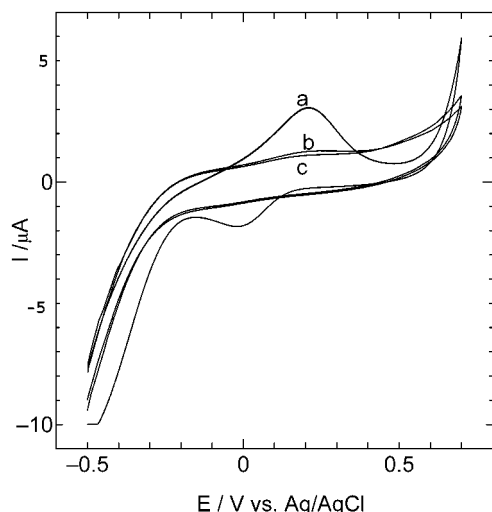
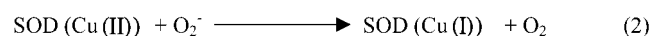
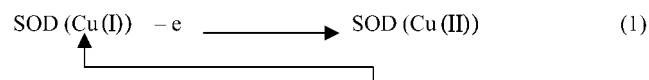


Figure 3. CVs obtained at (a) SOD/Cys/Au, (b) bare Au, and (c) Cys/Au electrodes in PBS ( $\text{O}_2$ -saturated) containing 0.002 unit of XOD and 50  $\mu\text{M}$  xanthine. Scan rate, 100  $\text{mV s}^{-1}$ .

electron transfer of SOD and its relevance to the redox reaction of the copper complex moiety in SOD formed a strong basis for the development of the SOD-based third-generation biosensor for  $\text{O}_2^-$  because the copper complex moiety has been well documented as the active site for the catalytic dismutation of  $\text{O}_2^-$ .<sup>41</sup>

Figure 3 shows CVs at the bare Au, Cys/Au, and SOD/Cys/Au electrodes in PBS ( $\text{O}_2$ -saturated) containing 0.002 unit of XOD and 50  $\mu\text{M}$  xanthine, i.e., in the presence of  $\text{O}_2^-$ . Both of the cathodic and anodic peak currents corresponding to the redox reaction of the SOD confined on the electrode are significantly increased, compared with those in the absence of  $\text{O}_2^-$  (Figure 1a). Such a redox response was not observed at the bare Au and Cys/Au electrodes in the presence of  $\text{O}_2^-$ . The large anodic and cathodic currents starting from about 600 and  $-300$  mV were due to the oxidation of UA and the reduction of  $\text{H}_2\text{O}_2$  and  $\text{O}_2$ , respectively.  $\text{H}_2\text{O}_2$  and UA are coproduced in the xanthine/XOD-based  $\text{O}_2^-$  generating system.<sup>47</sup> The observed increase in the anodic and cathodic current response of SOD/Cys/Au in the presence of  $\text{O}_2^-$  can be considered to result from the oxidation and reduction of  $\text{O}_2^-$ , respectively, which are effectively mediated by the SOD confined on the electrode. That is, the following reaction mechanism can explain the enhanced oxidation current observed in the anodic scan:



Similarly, the reduction current is enhanced in the cathodic scan according to the following scheme:

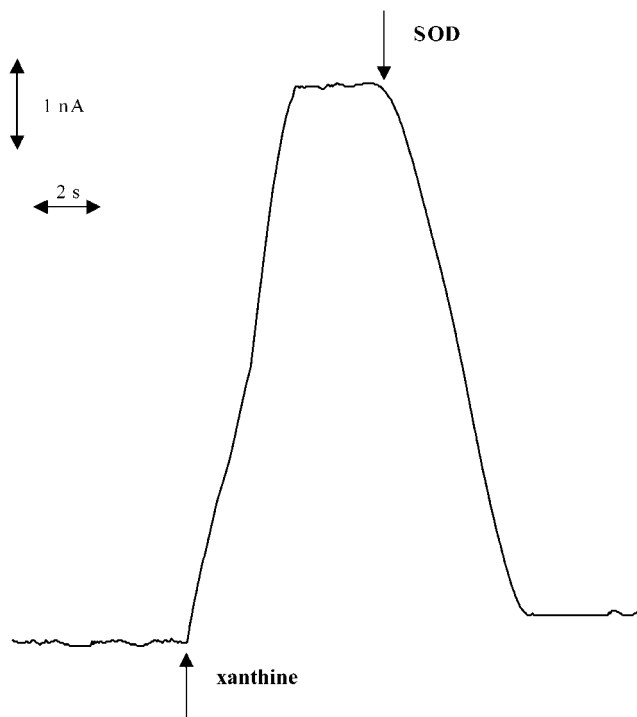


Figure 4. Typical current–time response obtained at SOD/Cys/Au in PBS ( $\text{O}_2$ -saturated) solution containing 0.002 unit of XOD upon the addition of 50 nM xanthine and the subsequent addition of 6  $\mu\text{M}$  SOD. The electrode was polarized at 300 mV, and the solution was gently stirred with a magnetic stirrer at 200 rpm.

To the best of our knowledge, this is the first observation of  $\text{O}_2^-$  being both oxidized and reduced at a SOD-based electrode. Such a bidirectional electromediation (electrocatalysis) by SOD/Cys/Au is essentially based on the inherent specificity of SOD for the dismutation of  $\text{O}_2^-$ ; i.e., SOD catalyzes both the reduction of  $\text{O}_2^-$  to  $\text{H}_2\text{O}_2$  and the oxidation to  $\text{O}_2$  via a redox cycle of its Cu complex moiety as well as the direct electron transfer of SOD we realized at Cys/Au. Thus, this coupling between the electrode and enzyme reactions of SOD could facilitate the development of the third-generation biosensor for  $\text{O}_2^-$ .

**Amperometric Response of SOD/Cys/Au to  $\text{O}_2^-$ .** By taking into account the possibility of both oxidation and reduction of  $\text{O}_2^-$  at SOD/Cys/Au, the electrode was polarized at 300 or  $-200$  mV for the measurement of  $\text{O}_2^-$ . Figure 4 shows the typical current–time response of SOD/Cys/Au at the applied potential of 300 mV on addition of xanthine and SOD to the  $\text{O}_2$ -saturated PBS containing 0.002 unit of XOD. After a stable background current was obtained under the applied potential conditions, 50 nM xanthine was pipetted into the PBS to generate  $\text{O}_2^-$ . The introduction of xanthine into the electrolyte solution produced a rapid and obvious increase in the anodic current. To verify that the observed anodic current is attributed to the oxidation of  $\text{O}_2^-$  rather than the coproducts of the XOD/xanthine-based  $\text{O}_2^-$  generating reaction, i.e., uric acid and  $\text{H}_2\text{O}_2$ , we added 6  $\mu\text{M}$  SOD to the solution since SOD, a selective scavenger of  $\text{O}_2^-$ , can specifically dismutate  $\text{O}_2^-$ . This addition caused the anodic current to decrease by  $>95\%$  within 6 s. More addition of SOD to the solution resulted in the anodic current decreased to almost the background current, strongly indicating that only  $\text{O}_2^-$  generated

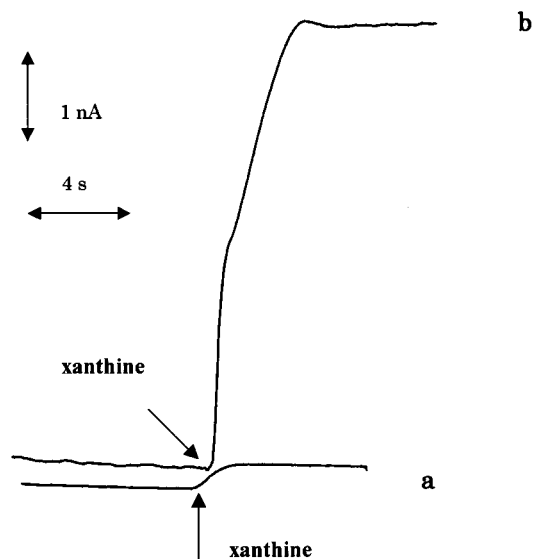


Figure 5. Current-time responses of (a) apo-SOD/Cys/Au and (b) SOD/Cys/Au toward  $O_2^-$  in PBS containing 0.002 unit of XOD upon the addition of 40 nM xanthine. Other conditions are the same as those in Figure 4.

by the XOD/xanthine system is concerned in the anodic current response measured at SOD/Cys/Au.

To examine the direct oxidation of  $O_2^-$  at SOD/Cys/Au without the above-mentioned redox mediation via SOD, the response of apo-SOD/Cys/Au toward  $O_2^-$  was also measured. The result is shown together with that of SOD/Cys/Au in Figure 5. With the addition of xanthine to the solution, a large anodic current was recorded at SOD/Cys/Au due to SOD-catalyzed oxidation of  $O_2^-$  as mentioned above, whereas much less response was obtained at apo-SOD/Cys/Au, indicating that the oxidation of  $O_2^-$  at SOD/Cys/Au was based on the SOD enzyme amplification. The minor current response observed at apo-SOD/Cys/Au may be considered to be due to the direct oxidation of  $O_2^-$ , independent of the SOD catalytic dismutation, probably because of the small size of  $O_2^-$  and its permeation through the apo-SOD/cysteine layer and the pinhole of cysteine monolayer. The formal potential of the  $O_2/O_2^-$  redox couple is  $-0.31$  V versus Ag/AgCl.<sup>49</sup> and thus, this direct oxidation of  $O_2^-$  may occur at ordinary electrodes at not so positive potentials and thus is common to most kinds of amperometric  $O_2^-$  biosensors, e.g., Cyt. *c*-based  $O_2^-$  sensor.<sup>24</sup> It should be mentioned that the ratio of the oxidation current of  $O_2^-$  obtained via SOD enzyme amplification to its direct oxidation current should be higher than that at the Cyt. *c*-based  $O_2^-$  sensor<sup>24</sup> because the catalytic activity of SOD is several hundred times higher than that of Cyt. *c* and the specificity of SOD toward  $O_2^-$  is also significant (vide infra).

Superior to previous enzyme sensors for  $O_2^-$  detection,<sup>20,23,24,26–29,31,32,36,38</sup>  $O_2^-$  could also be detected with SOD/Cys/Au by utilizing the catalytic activity of SOD toward the reduction of  $O_2^-$  to  $H_2O_2$ , as mentioned above. The typical current-time response obtained at SOD/Cys/Au at  $-200$  mV is shown in Figure 6. The addition of xanthine to the solution resulted in an obvious increase in the cathodic current, but such a cathodic current was not observed at the bare Au and Cys/Au

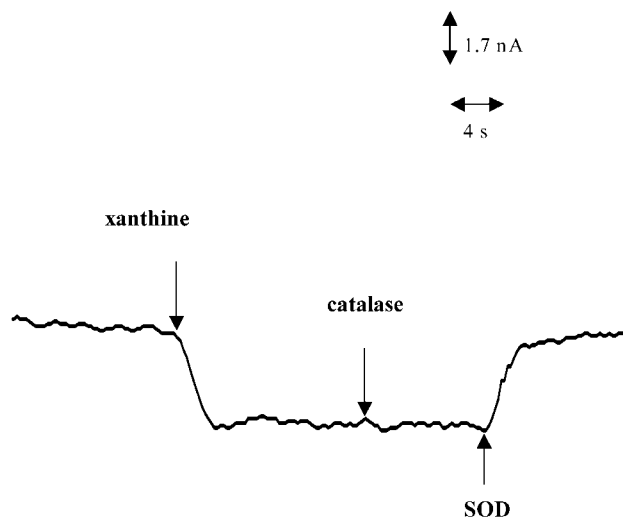


Figure 6. Typical current-time responses obtained at SOD/Cys/Au in PBS solution ( $O_2$ -saturated) containing 0.002 unit of XOD upon the addition of 30 nM xanthine and the subsequent addition of 590 units of catalase and 6  $\mu$ M SOD. The electrode was polarized at  $-200$  mV, and other conditions are the same as those in Figure 4.

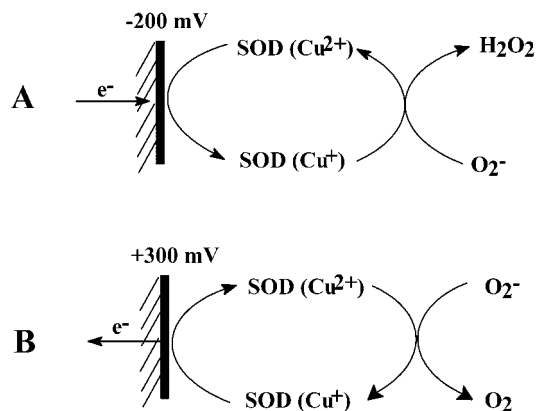


Figure 7. Amperometric response of SOD/Cys/Au to  $O_2^-$  based on the catalytic reduction (A) and oxidation (B) of  $O_2^-$  by SOD.

electrodes. As can be seen from Figure 6, the introduction of catalase, which has a high catalytic activity toward the dismutation of  $H_2O_2$ , to the solution did not result in any change in the current response, suggesting that the observed cathodic current is not the reduction of  $H_2O_2$  coproduced in the XOD/xanthine-based  $O_2^-$  generating reaction. On the contrary, the addition of SOD caused the cathodic current to decrease to the background level. Thus, the observed cathodic response is ascribable to the reduction of  $O_2^-$  mediated by the SOD confined on the electrode.

The two pathways (i.e., anodic and cathodic processes) of the response of SOD/Cys/Au to  $O_2^-$  through the recognition and amplification by SOD could be schematically illustrated in Figure 7.

**Potential Dependence.** Figure 8 displays the potential dependence of amperometric response of SOD/Cys/Au to  $O_2^-$  in PBS. The current increased with increasing positive operating potential and reached a plateau at greater than  $\sim 300$  mV. The anodic current was found to increase greatly at potentials higher than  $\sim 600$  mV due to the oxidation of uric acid coproduced from the XOD/xanthine-based  $O_2^-$  generating system (data not shown). On the other hand, the cathodic current increased with negative

(49) Matsumoto, F.; Tokuda, K.; Ohsaka, T. *Electroanalysis* **1996**, *8*, 648–653.

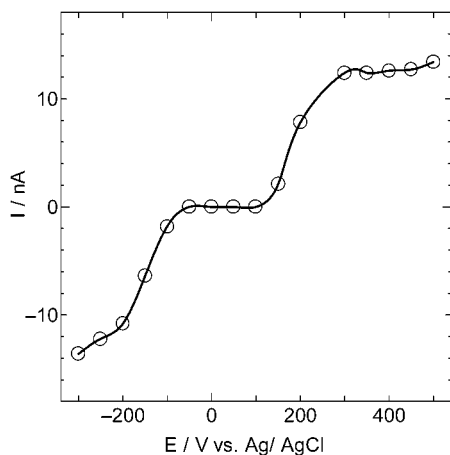


Figure 8. Potential dependence of the amperometric response of SOD/Cys/Au toward  $26 \text{ nM min}^{-1} \text{ O}_2^-$  in PBS ( $\text{O}_2$ -saturated) containing 0.002 unit of XOD and 100 nM xanthine. The solution was stirred with a magnetic stirrer at 200 rpm.

shift of the operating potential. At potentials more negative than  $\sim -200 \text{ mV}$ , the cathodic current increased sharply due to the reduction of  $\text{O}_2$  in PBS and  $\text{H}_2\text{O}_2$  produced from the  $\text{O}_2^-$  generating system. This current–potential profile gives the experimental basis for choosing the operating potential suitable for the measurement of  $\text{O}_2^-$  using SOD/Cys/Au. As mentioned above, the present sensor allows us to measure  $\text{O}_2^-$  by polarizing the electrode both anodically and cathodically; typically, the electrode was polarized at 300 and  $-200 \text{ mV}$ .

**Linear Range and Detection Limit.** Amperometric responses of SOD/Cys/Au to successive concentration changes of  $\text{O}_2^-$  were examined at the applied potentials of 300 and  $-200 \text{ mV}$ , and the obtained current–time responses are shown in Figure 9. Well-defined steady-state current responses were obtained at both 300 and  $-200 \text{ mV}$ , and the currents increased stepwise with successive additions of xanthine. The generated  $\text{O}_2^-$  can undergo spontaneous dismutation into  $\text{O}_2$  and  $\text{H}_2\text{O}_2$  under the experimental conditions. The counterbalance between the generation of  $\text{O}_2^-$  and its degradation results in a constant equilibrium concentration of  $\text{O}_2^-$ . The calibration plots obtained from Figure 9 are shown in Figure 10. The steady-state currents at 300 and  $-200 \text{ mV}$  were proportional to the rate of  $\text{O}_2^-$  generation in the examined range of  $\sim 13\text{--}130 \text{ nM min}^{-1}$ . The sensitivity of SOD/Cys/Au was found to be 24 and  $22 \text{ nA cm}^{-2}/(\text{nM min}^{-1})$  at 300 and  $-200 \text{ mV}$ , respectively. The detection limit was evaluated based on a signal-to-noise ratio of 3:1 and calculated to be 5 nM at 300 mV and 6 nM at  $-200 \text{ mV}$ , respectively. The response time of the sensor was measured as the time to reach 95% of the maximum change in response to a step injection of xanthine and found to be less than 6 s. For the stability test, the anodic and cathodic responses for  $\text{O}_2^-$  generated by the XOD/xanthine system were recorded four times each day and the current responses were found to be constant for at least one week. In addition, we have found that the deviation of the current responses of 10 sensors prepared with the same method did not exceed 5%.

**Interference.** The main purpose for the development of  $\text{O}_2^-$  sensor lies in monitoring  $\text{O}_2^-$  in biological systems. As reported previously,<sup>24</sup> there are a variety of interferences coexisting in biological samples, suggesting that the sensor used for the

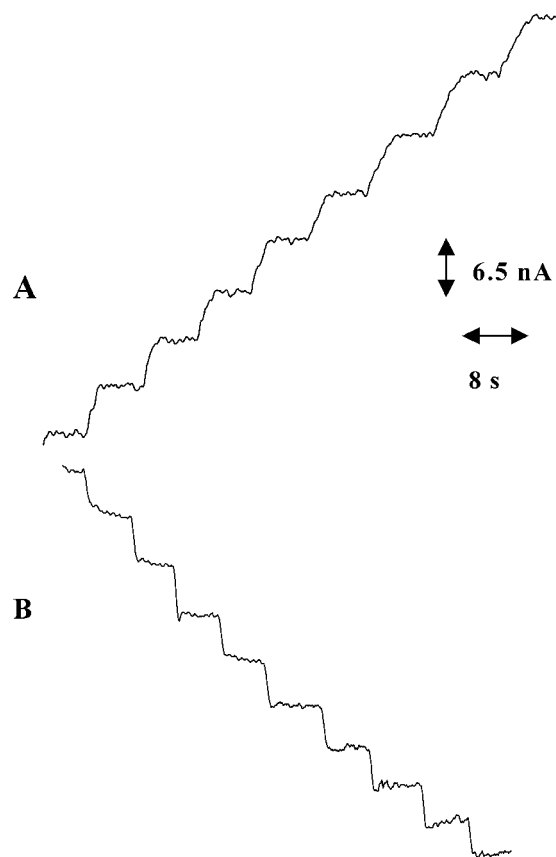


Figure 9. Typical steady-state current–time responses of SOD/Cys/Au at (A) 300 and (B)  $-200 \text{ mV}$  in PBS ( $\text{O}_2$ -saturated) containing 0.002 unit of XOD upon successive addition of 50 nM xanthine. The solution was stirred with a magnetic stirrer at 200 rpm.

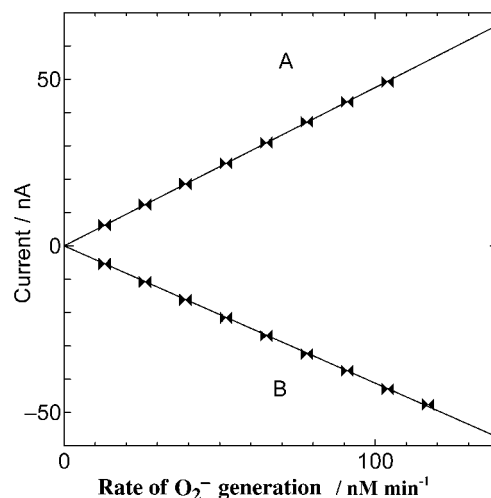


Figure 10. Calibration plots of the anodic (A) and cathodic (B) steady-state currents against the concentration of  $\text{O}_2^-$ . The data (A) and (B) were taken from Figure 9A and B, respectively.

practical measurements should have significant specificity against potential interferences. In biological systems, as mentioned above,  $\text{H}_2\text{O}_2$  is a metabolite in the degradation of  $\text{O}_2^-$  and a product of enzyme reactions of endogenous oxidases such as monoamine oxidase and L-amino acid oxidase. In addition,  $\text{H}_2\text{O}_2$  is one of the main byproducts in the XOD/xanthine system to generate  $\text{O}_2^-$ . Therefore, the specificity of the sensor against  $\text{H}_2\text{O}_2$  is of great importance in its application for the determination of  $\text{O}_2^-$  in

Table 1. Current Responses of the SOD/Cys/Au Electrode for the Estimation of  $O_2^-$  against the Potential Interferences

interferences (concentration)	current/nA <sup>a</sup>	
	300 mV	200 mV
$O_2^-$ (13 nM min <sup>-1</sup> ) <sup>b</sup>	6.2 (100)	-5.4 (100)
H <sub>2</sub> O <sub>2</sub> (20 $\mu$ M) <sup>c</sup>	0 (0)	-0.09 (1.7)
5-HIAA (10 $\mu$ M) <sup>c</sup>	0 (0)	-0.004 (0.07)
HVA (10 $\mu$ M) <sup>c</sup>	0 (0)	-0.002 (0.03)
DOPAC (10 $\mu$ M) <sup>c</sup>	0.03 (0.48)	0 (0)
UA (50 $\mu$ M) <sup>c</sup>	1.2 (19)	0 (0)
AA (500 $\mu$ M) <sup>c</sup>	2.3 (37)	0 (0)

<sup>a</sup> The values given in parentheses are percentages with respect to the current for  $O_2^-$  at the applied electrode potentials of 300 and -200 mV vs Ag/AgCl. <sup>b</sup> Anodic (positive values) and cathodic (negative values) currents observed on the addition of 50 nM xanthine into 25 mM PBS (pH 7.4,  $O_2$  saturated) containing 0.002 unit of XOD. The rate of  $O_2^-$  generation is 13 nM min<sup>-1</sup>. The solution was stirred with a magnetic stirrer at 200 rpm. <sup>c</sup> Anodic (positive values) and cathodic (negative values) currents observed on the addition of 20  $\mu$ M H<sub>2</sub>O<sub>2</sub>, 10  $\mu$ M 5-HIAA, 10  $\mu$ M HVA, 10  $\mu$ M DOPAC, and 50  $\mu$ M UA or 500  $\mu$ M AA into 25 mM PBS (pH 7.4). The solution was stirred with a magnetic stirrer at 200 rpm.

biological systems as well as in its calibration. Thus, the interference from H<sub>2</sub>O<sub>2</sub> was first examined. In addition, the current responses of SOD/Cys/Au against other potential interferences such as the principal metabolites (DOPAC, HVA, and 5-HIAA) of some neurotransmitters, AA, and UA were also investigated. Table 1 summarizes the steady-state current responses of SOD/Cys/Au to these interferences in comparison with those measured for  $O_2^-$  at 300 and -200 mV, in which the concentrations of the interferences approximate their ECF levels.<sup>50,51</sup> As seen from Table 1, no current response for H<sub>2</sub>O<sub>2</sub> was observed at SOD/Cys/Au at 300 mV and the response was also negligible at -200 mV. This point is remarkable in comparison with the Cyt. c-based  $O_2^-$  sensor; that is, it shows a good response for H<sub>2</sub>O<sub>2</sub> because of the peroxidase activity of Cyt. c.<sup>24</sup> In other words, interference from H<sub>2</sub>O<sub>2</sub> cannot be avoided at a Cyt. c-based  $O_2^-$  sensor. AA is another

major interference perplexing most electrochemical techniques for biological measurements because of its high concentration and low oxidation potential. At 300 mV, the interference level of 37% was obtained for AA, indicating that further improvement will be needed to enhance the specificity of the sensor for  $O_2^-$  determination in the presence of a high concentration of AA. To the contrary, no response of AA was obtained at -200 mV. In addition, we found that UA is the interfering agent for the measurement of the oxidation current of  $O_2^-$  at 300 mV (the degree of its interference is 19%), but the interference of 5-HIAA, HVA, and DOPAC is negligible at both 300 and -200 mV. Thus, the present sensor has a bright prospect for the selective and sensitive detection of  $O_2^-$  in biological systems.

## CONCLUSIONS

By utilizing the strategy of the direct electrochemistry of SOD promoted by cysteine, we developed a third-generation amperometric biosensor for the measurement of  $O_2^-$ . The present sensor had good sensitivity and selectivity, a rapid response time, excellent linearity at nanomolar  $O_2^-$  concentrations, good durability, and a low detection limit. In addition, this sensor allowed us to measure  $O_2^-$  by polarizing the electrode both anodically and cathodically. This is of the great advantage in the measurement of  $O_2^-$ , especially in biological systems, because we can suitably choose the operating potential by taking into account the potential interferences. The obtained results demonstrate that the present sensor is very promising for the durable and reliable measurement of  $O_2^-$  in biological systems.

## ACKNOWLEDGMENT

The present work was financially supported by Grant-in-Aids for Scientific Research (12875164) and Scientific Research (A) (10305064) from the Ministry of Education, Science, Sports, Culture and Technology, Japan. Y.T. thanks the Government of Japan for the Monbu-Kagaku sho scholarship.

Received for review December 9, 2001. Accepted March 14, 2002.

AC0157270

(50) Miele, M.; Fillenz, M. J. *Neurosci. Methods* **1996**, *70*, 15-19.

(51) Zetterstrom, T.; Vernet, L.; Ungerstedt, U.; Jonzon, T. B.; Fredholm, B. B. *Neurosci. Lett.* **1982**, *29*, 111-115.